Saudi Pharmaceutical Journal 31 (2023) 101818

HOSTED BY

Contents lists available at ScienceDirect

Saudi Pharmaceutical Journal

journal homepage: www.sciencedirect.com

Original article

Prunetin in a GPR30-dependent manner mitigates renal ischemia/reperfusion injury in rats via interrupting indoxyl sulfate/TLR4/TRIF, RIPK1/RIPK3/MLKL, and RIPK3/PGAM5/DRP-1 crosstalk

Ahmed B. Hamed [a], Hanan S. El-Abhar [a], Dalaal M. Abdallah [b,*], Kawkab A. Ahmed [c], Yasmin S. Abulfadl [a]

[a] Department of Pharmacology, Toxicology, and Biochemistry, Faculty of Pharmacy, Future University in Egypt, Cairo 11835, Egypt
[b] Department of Pharmacology and Toxicology, Faculty of Pharmacy, Cairo University, Cairo 11562, Egypt
[c] Department of Pathology, Faculty of Veterinary Medicine, Cairo University, Giza 12211, Egypt

ARTICLE INFO

Article history:
Received 18 July 2023
Accepted 2 October 2023
Available online 5 October 2023

Keywords:
Prunetin
Ischemia/reperfusion
GPR30
RIPK1/RIPK3/MLKL
Caspase-8
PGAM5/DRP-1

ABSTRACT

The potential health benefits of phytochemicals in preventing and treating diseases have gained increasing attention. Here, we proved that the methylated isoflavone prunetin possesses a reno-therapeutic effect against renal ischemia/reperfusion (I/R) insult by activating G protein-coupled receptor 30 (GPR30). After choosing the therapeutic dose of prunetin against renal I/R injury in the pilot study, male Sprague Dawley rats were allocated into 5 groups; viz., sham-operated (SO), SO injected with 1 mg/kg prunetin intraperitoneally for three successive days, untreated I/R, I/R treated with prunetin, and I/R treated with G-15, the selective GPR30 blocker, followed by prunetin. Treatment with prunetin reversed the I/R renal injury effect and majorly restored normal renal function and architecture. Mechanistically, prunetin restored the I/R-induced depletion of renal GPR30, an impact that was canceled by the pre-administration of G-15. Additionally, post-administration of prunetin normalized the boosted inflammatory markers indoxyl sulfate, TLR4, and TRIF and abrogated renal cell demise by suppressing necroptotic signaling, verified by the inactivation of p-RIPK1, p-RIPK3, and p-MLKL while normalizing the inhibited caspase-8. Besides, prunetin reversed the I/R-mediated mitochondrial fission by inhibiting the protein expression of PGMA5 and p-DRP-1. All these favorable impacts of prunetin were nullified by G-15. To sum up, prunetin exhibited a significant reno-therapeutic effect evidenced by the enhancement of renal morphology and function, the suppression of the inflammatory cascade indoxyl sulfate/TLR4/TRIF, which turns off the activated/phosphorylated necroptotic trajectory RIPK1/RIPK3/MLKL, while enhancing caspase-8. Additionally, prunetin opposed the mitochondrial fission pathway RIPK3/PGMA5/DRP-1, effects that are mediated via the activation of GPR30.

1. Introduction

Renal ischemia/reperfusion (I/R) injury stands as a prominent causative factor for acute kidney injury (AKI), a severe clinical condition marked by a sudden deterioration in renal function (Lattanzio and Kopyt, 2009). Apart from being one of the consequences of cardiac surgeries, I/R is observed in various clinical cases, such as sepsis, and renal transplantation (Bonventre and Weinberg, 2003). Experimentally, renal I/R is a well-established model that resembles the human pathophysiological situation and allows for examining the beneficial roles of various drugs on renal functions (Shiva et al., 2020).

Although activating the nuclear estrogen receptors showed positive impacts on alleviating the renal I/R ailment (Satake et al., 2008; Ren et al., 2022), an earlier study stated that mitigation of

Abbreviations: AKI, Acute kidney injury; BUN, Blood urea nitrogen; DMSO, Dimethyl sulfoxide; GPR30, G protein-coupled receptor 30; I/R, Ischemia/reperfusion; PGAM5, Phosphoglycerate mutase 5; *p*-DRP-1, Phosphorylated dynamin-related protein 1; *p*-MLKL, Phosphorylated mixed lineage kinase domain-like; *p*-RIPK1, Phosphorylated receptor-interacting protein kinase 1; *p*-RIPK3, Phosphorylated receptor-interacting protein kinase 3; Pru, Prunetin; SO, Sham-operated; TLR4, Toll-like receptor 4; TBST, Tris-buffered saline provided with 0.1% Tween-20; TRIF, Toll/interleukin-1 receptor-domain-containing adaptor inducing interferon-beta.

* Corresponding author at: Department of Pharmacology and Toxicology, Faculty of Pharmacy, Cairo University, Kasr El-Aini Str., Cairo 11562, Egypt.
E-mail address: dalaal.abdallah@pharma.cu.edu.eg (D.M. Abdallah).

Peer review under responsibility of King Saud University.

ELSEVIER Production and hosting by Elsevier

https://doi.org/10.1016/j.jsps.2023.101818
1319-0164/

this insult could be independent of these receptors (Hutchens et al., 2010). This urged researchers to scrutinize the possible role of the membrane-bound G protein-coupled estrogen receptor 30 (GPR30), detected in 1997 (Carmeci et al., 1997), in improving renal I/R. (Chang et al., 2019) reported that activating this receptor may enhance renal vascular function by increasing nitric oxide content to protect against renal I/R insult. Apart from its presence in renal blood vessels, this receptor is also highly expressed in the pelvis and tubular epithelial cells (Zimmerman et al., 2016). Contrariwise to the classic nuclear estrogen receptors, stimulation of GPR30 induces rapid cellular signaling events, such as kinase activation and calcium mobilization, and it appears to regulate rapid transcriptional activation of specific genes (Prossnitz and Maggiolini, 2009). Besides, in a cerebral ischemia model, activated GPR30 possessed an anti-inflammatory effect via diminishing toll-like receptor 4 (TLR4) expression (Zhang et al., 2018).

Renal tubular epithelial cells and mesangial cells are known to express TLR4, and their expression is highly increased during renal I/R injury (Habib, 2021). Activation of TLR4 is implicated in multiple signaling pathways, including the induction of necroptosis (Grootjans et al., 2017). Necroptosis is a recently identified form of regulated cell death that induces innate immune responses by rupturing the damaged cells and releasing the intracellular components (Linkermann and Green, 2014). This type of cell demise is characterized by combining the features of necrosis and apoptosis (Dhuriya and Sharma, 2018). While necroptosis mimics the unrestricted morphological characteristics of necrosis (Belizario et al., 2015), it shares with apoptosis the controlled manner of cell death that is directed by the state of caspase-8 (Park et al., 2021). If caspase-8 is activated, it directs cell termination towards the extrinsic type of apoptosis; however, when the function of caspase-8 is hampered, TLR4 recruits/activates toll/interleukin-1 receptor-domain-containing adaptor inducing interferon-beta (TRIF), which triggers necroptosis and commences a cascade of events leading to necrosome formation (Holler et al., 2000; Liu et al., 2022).

The primary components of the activated classical necrosome are phosphorylated/ stimulated receptor-interacting protein kinase 1 (p-RIPK1) and p-RIPK3, which heterodimerize to facilitate the activation of the necroptosis executor mixed lineage kinase domain-like (MLKL) by RIPK3 to form the active/phosphorylated RIPK1/RIPK3/MLKL necrosome complex (Wang et al., 2014). Besides resulting in cell swelling and death, this complex can trigger mitochondrial fission by activating phosphoglycerate mutase 5 (PGAM5), which consequently activates dynamin-related protein 1 (DRP-1), resulting in mitochondrial fragmentation (Sang et al., 2023) to boost the necroptosis cue in a vicious cycle again (Wang et al., 2012). Moreover, a non-classical necrosome can result from the interaction between TRIF and RIPK3, which recruits and phosphorylates its downstream substrate/necroptosis executioner, MLKL (Dhuriya and Sharma, 2018). Indeed, the connivance of necroptotic machinery in the occurrence of renal I/R insult has been documented previously (Linkermann et al., 2012; Jun et al., 2020), indicating that necroptosis could be a probable therapeutic goal in limiting renal I/R insult.

Naturally occurring flavonoids have been reported for their therapeutic roles against various diseases through their pleiotropic mechanisms (Mutha et al., 2021). Prunetin is a 7-o-methylated isoflavone that showed the aptitude to promote bone regeneration via the activation of GPR30 (Khan et al., 2015). Besides, this isoflavone proved its anti-inflammatory potential by inhibiting TLR4 in the human nasal epithelium (Hu and Li, 2018) and showed several beneficial roles against tissue injury in various experimental models, mainly through its potent antioxidant and anti-inflammatory activities (Li et al., 2022a; Yang et al., 2013).

As reviewed, the possible therapeutic mechanism(s) of activating GPR30 in the renal I/R model still need to be fully divulged. Moreover, neither the impact of prunetin on kidney injury nor its role in activating renal GPR30 was studied before. To fill this knowledge gap, our goal and hypothesis in this study are to reveal the reno-therapeutic potential of prunetin against I/R-induced AKI in rats and whether its anti-necroptotic/anti-inflammatory activities are mediated through the activation of GPR30 using the corresponding blocker.

2. Material and methods

2.1. Drugs and chemicals

Prunetin, ketamine, and xylazine were purchased from Sigma-Aldrich (M.O., U.S.A.), whereas G-15 was obtained from Tocris Bioscience (Abingdon, U.K.). Before administration, each of prunetin and G-15 was dissolved in a 3 % dimethyl sulfoxide (DMSO) solution.

2.2. Animals

Adult male Sprague Dawley rats (200–250 g) were procured from El-Nile Co. (Cairo, Egypt). Before experimentation, rats were maintained under controlled conditions (humidity level of 65 ± 5, 12/12 h dark/light cycle, room temperature of 23 ± 2 °C) in the animal house of the Faculty of Pharmacy, Future University in Egypt (Cairo, Egypt) for one week. All animals had free access to water and a standard diet, and all procedures and manipulations of these animals complied with the guidelines established by the Guide for the Care and Use of Laboratory Animals (Nih and Oer, 2011). The Research Ethics Committee at the Faculty of Pharmacy, Cairo University, Cairo, Egypt, approved the study protocol (Permit Number: PT 2792).

2.3. Induction of renal I/R

The overnight fasting animals were anaesthetized by ketamine/xylazine (75/8 mg/kg; i.p.; (Nuransoy et al., 2015)) and were then placed in a supine position on a 37 °C heated pad to maintain body temperature during the operation. After a midline abdominal incision, the renal pedicles were clamped bilaterally to induce renal ischemia, as indicated by the immediate discoloration of the kidneys. After 45 min, the pedicles were declamped to permit reperfusion for 24 h. Finally, the abdominal incision was sutured, and the animals were observed during their recovery from anesthesia (Ragab et al., 2014).

2.4. Experimental design

Since no fixed dose for prunetin was available for the kidney I/R model, a pilot study was conducted to determine the effective dose. For this preliminary study, animals (n = 20) were divided into five groups, with four animals assigned to each group. Sham-operated rats (SO; group 1) were administered the vehicle (3 % DMSO) after being subjected to all processes of the I/R operation except for the occlusion of the renal pedicles. The animals of the other four groups underwent the complete steps of I/R surgery; in group 2, animals were injected only with DMSO, while those in groups 3–5 received different doses of prunetin (Khan et al., 2015), whereas in group 3, rats were injected with 0.25 mg/kg, while groups four and five received 0.5 mg/kg and 1 mg/kg, respectively. All treatments were injected intraperitoneally daily (once/-day) for a continuous duration of three days.

Since the highest dose (1 mg/kg) showed the best effect, it was chosen in the second part of the study to assess the renotherapeutic mechanism(s) of prunetin against I/R-induced AKI. In this part, forty rats were randomized into five groups (n = 8 each); animals in the first group served as the SO control group and received the vehicle, whereas those in the second group mimicked the SO group but were injected with prunetin (1 mg/kg, i.p.). Rats in the 3 remaining groups underwent renal I/R; those in groups 3 and 4 were injected with the vehicle to be designated as the I/R model or treated with 1 mg/kg prunetin (i.p.) to serve as the treated group, respectively. Finally, animals in the 5th group received the GPR30 blocker, G-15 (50 μg/day, s.c.; **(**Lu et al., 2013**)**), 25 min before each prunetin injection. All treatments were injected once daily for three consecutive days.

2.5. Sample preparation

For the first part of the study, all animals were weighed and then blood was withdrawn from the tail vein 24 h after the last dose of prunetin. Blood was used to separate serum for the evaluation of renal function biomarkers. The cervical dislocation was then used for the euthanasia of the anesthetized rats, and their kidneys were harvested, washed, and weighed to determine the renal index.

In the core study, blood samples were collected to determine the serum level of the uremic toxin indoxyl sulfate, and the assembled kidneys were used to examine the histopathological alterations, where the right kidneys of 3 animals/group were kept in 10 % formal saline. For Western blot analysis, the right kidneys of another three rats were suspended in RIPA buffer/complete protease inhibitor to quantify total protein. The left kidneys of 4 animals were retained in ribonucleic acid (RNA) later solution (Thermo Fisher Scientific, M.A., U.S.A.) to analyze GPR30 using the quantitative real-time polymerase chain reaction (qRT-PCR) technique. Finally, for enzyme-linked immunosorbent assay (ELISA) assessment, the remaining kidneys (2 right and 4 left) were placed in phosphate-buffered saline to be homogenized.

2.6. Assessment of kidney index

The weight of the kidney relative to the body weight was estimated using the following equation:

$$(Kidney\ weight/body\ weight)x100$$

2.7. Assessment of renal function biomarkers

Serum levels of the standard kidney function parameters, viz., blood urea nitrogen (BUN; Stanbio, TX, U.S.A.; CAT # 2020–430) and creatinine (Randox, Crumlin, U.K.; CAT # CR510), were assayed calorimetrically according to the manufacturer protocol.

2.8. qRT-PCR assay

To assess the gene expression of renal GPR30, the GeneJET RNA Purification Kit obtained from Thermo Fisher Scientific (# K0731) was utilized to extract total RNA from kidney tissues. The purity of the RNA was determined spectrophotometrically by measuring the A260/A280 ratio. Following, the reverse transcription of RNA into complementary deoxyribonucleic acid (cDNA) was performed using the RevertAid First Strand cDNA Synthesis Kit (Thermo Fisher Scientific; # K1622). For qRT-PCR analysis, the Qiagen rotor gene Q6 Plex RT-PCR system (Qiagen, Germany) was employed, according to the previously described method **(**Abulfadl et al., 2018**)**. A 25 μl reaction mixture containing Maxima SYBR Green/ROX qPCR Master Mixes (# K0221; Thermo Fisher Scientific) was used with triplicate analyses for robustness. Primer sequences and accession numbers are duly documented in Table 1**.** Efficiency evaluation employed the ΔCt method, and data was analyzed using Rotorgene Q software with the automatic Ct setting to determine baseline and threshold values. The relative expression level of each gene after normalization to β-actin was calculated using the $2^{-\Delta\Delta Ct}$ formula.

2.9. ELISA assay

The serum level of indoxyl sulfate was estimated using the corresponding kit procured from MyBioSource (C.A., U.S.A.; # MBS3809027). The ELISA kits used for the assessment of renal contents of GPR30 (# MBS1600698), TLR4 (# CSB-E15822r), and TRIF (# ABIN6265566) were purchased from MyBioSource, CUSABIO (T.X., U.S.A.), and Antibodies-online Inc. (P.A., U.S.A.), respectively. All procedures followed the protocols provided by the manufacturers.

2.10. Western blotting

The assessment of the target proteins in the nucleus, mitochondria, or cytosol was performed using the Abcam (C.B., U.K.) fractionation kit (# ab109719), whereas the BCA assay kit (Bio-Rad, C.A., U.S.A.) was used to estimate the extracted fractions' protein contents. SDS-PAGE (10 % gel) was used to separate equal aliquots of protein (20 μg/lane) from each sample to be later transferred into polyvinylidene fluoride (PVDF) membranes (Thermo Fisher Scientific). The latter were treated with bovine serum albumin (5 %) in Tris-buffered saline/ 0.1 % Tween-20 (TBST) at room temperature (25 °C) for 40 min, followed by probing the blocked membrane with the corresponding primary antibodies at 4 °C overnight. The primary antibodies against the cytosolic parameters were cleaved caspase-8 (# ab25901; Abcam), *p*(ser166)-RIPK1 (# 53286; Cell Signaling Technology, MA, USA), total RIPK1 (# 3493; Cell Signaling Technology), *p*(ser232)-RIPK3 (# MBS9429436; MyBioSource), total RIPK3 (# 15828; Cell Signaling Technology), *p*(ser345)-MLKL (# MBS9431094; MyBioSource), and total MLKL (# ab243142; Abcam). In addition, other antibodies were used to assess the mitochondrial content of PGAM5 (# MBS9612114; MyBioSource), *p*(ser616)-DRP-1 (# 3455; Cell Signaling Technology), and total DRP-1 (# 8570; Cell Signaling Technology). The membranes were then incubated for 2 h at room temperature with HRP-labeled secondary antibody (# ab97057; Abcam) after rinsing with TBST 5 times. The ECL detection kit (# ab65623; Abcam) was used to visualize the expressed proteins of interest, and the intensity of the bands was assessed after being normalized to β-actin.

2.11. Histopathological assessment of AKI

Following formalin decantation, kidney tissues were processed by the paraffin embedding technique. The paraffin blocks were sectioned transversely (5 μm), and the sections were placed on glass slides, deparaffinized, stained with Hematoxylin and Eosin (H&E), and examined under a light microscope (BX43, Olympus, Tokyo, Japan) blindly by a pathologist. The examined sections were pho-

Table 1
Sequences of primers and accession numbers.

Target Gene	Sequences	Accession number
GPR30	Forward: 5′-TCTACCTAGGTCCCGTGTGG-3′ Reverse: 5′-AGGCAGGAGAGGAAGAGAGC-3′	NM_133573
β-Actin	Forward: 5′-CCCATCTATGAGGGTTACGC-3′ Reverse: 5′-TTTAATGTCACGCACGATTTC-3′	NM_031144.3

tographed using the CellSens dimension software (Olympus) connected to the Olympus DP27 camera.

The scoring system from 0 to 5 adopted from a previous study (Mansour et al., 2022) was used to assess renal histopathological injury in six distinct microscopic fields per animal (n = 3/group). The scoring was based on the percentage of renal damage observed: 0 represented normal condition, 1 indicated mild damage (<10 %), 2 denoted moderate damage (10–25 %), 3 represented severe damage (>25–50 %), 4 indicated very severe damage (>50–75 %), and 5 represented extensive damage (>75 %).

2.12. Statistical analysis

For data analysis, parametric results were analyzed using one-way analysis of variance (ANOVA) followed by Tukey's post-hoc test, and the results were presented as mean ± standard deviation (S.D.). Non-parametric data were analyzed using the Kruskal-Wallis test followed by Dunn's post-hoc test, and the results were presented as medians (minimum–maximum). A significance level of 0.05 was used as the threshold for determining statistical significance. GraphPad Prism version 8.0 (GraphPad Software, CA, U.S.A.) was employed for all statistical analyses.

3. Results

3.1. The impact of different doses of prunetin on renal function biomarkers and kidney index in rats with I/R

As compared to the SO group, Fig. 1 revealed that the I/R insult provoked kidney injury manifested by boosted serum levels of **(A)** BUN and **(B)** creatinine. On the other hand, treatment with prunetin 1 mg/kg significantly improved kidney function compared to the I/R group and returned the heightened BUN and creatinine serum levels to their normal levels. The effect of the high dose was significant on the lower doses, viz., 0.25 mg/kg and 0.5 mg/kg, which failed to alter the I/R effect. In the same pattern, the **(C)** kidney index was markedly elevated in the I/R group relative to the SO group, but post-administration of prunetin 1 mg/kg prominently normalized it. This effect significantly overrode that of prunetin 0.25 mg/kg and 0.5 mg/kg, which did not affect this index relative to the I/R group.

Since the core study recorded no significant difference between the SO and the SO treated with prunetin in all the assessed parameters, the comparison was related to the untreated SO group.

3.2. Prunetin increased the renal expression and content of GPR30 in rats with I/R

The I/R insult has a sharply downregulated effect on the renal mRNA expression of GPR30, as depicted in Fig. 2 **(A)** relative to the SO group. However, this effect was markedly reversed after the post-injection of prunetin (1 mg/kg) to reach its normal level, an effect that was completely canceled when prunetin was preceded by the GPR30 blocker G-15. Similarly, the I/R insult **(B)** abated the GPR30 protein content, but treatment with prunetin returned it to a non-significant level from the control. Nevertheless, this beneficial effect was nullified by G-15 pre-injection.

3.3. Prunetin lessened indoxyl sulfate in the serum besides the renal contents of TLR4 and TRIF in a GPR30-dependent manner in rats exposed to I/R

Relative to the SO group, the I/R insult signified its inflammatory effect (Fig. 3**)**, evidenced by the upsurge of the uremic toxin **(A)** indoxyl sulfate in serum besides the renal contents of **(B)** TLR4 and **(C)** TRIF. Meanwhile, treatment with prunetin significantly decreased the elevated markers with no significant difference from the SO group. To confirm that the effect of prunetin is GPR30-dependent, the presence of the blocker opposed the beneficial anti-inflammatory capacity of prunetin and returned the parameters to their I/R level.

3.4. Prunetin turned off the activated necroptosis signaling in rats with I/R

The I/R injury caused cellular death by necroptosis (Fig. 4), where the expressions of the necroptotic proteins **(A)** *p*-RIPK1, **(B)** *p*-RIPK3, and **(C)** *p*-MLKL were markedly bolstered, whereas the renal expression of **(D)** cleaved caspase-8 was almost depleted in comparison with the SO group. Conversely, prunetin proved its anti-necroptotic aptitude by markedly diminishing the expression of the necroptotic proteins and normalizing that of caspase-8. These effects are induced by the activation of GPR30 since animals receiving prunetin preceded by G-15 showed no significant difference in the necroptotic markers relative to the I/R group.

3.5. Prunetin amended mitochondrial fission by downregulating PGAM5/DRP-1 nexus in rats with I/R

Fig. 5 illustrates the markedly amplified protein expression of the mitochondrial fission/necroptotic markers **(A)** PGAM5 and **(B)** ***p*-**DRP-1 in the I/R insulted rats relative to the SO group. Inversely, treatment with prunetin leveled off the protein expression of the two biomarkers, exhibiting no significant distinctions from the SO group. This effect depends on the activation of the membrane-bound estrogen receptor as proven by the nullified action of prunetin when preceded by the G-15 blocker. The latter effect brought these biomarkers to the I/R level.

3.6. Prunetin restored the altered histological structure of the kidney

The photomicrographs of the treated and untreated groups are presented in Fig. 6**.** As compared to the normal structure of **(A)** SO and **(B)** prunetin-treated SO groups, the **(C)** insulted rats show remarkable histopathological damage. The damage prominently affects the epithelial lining of renal tubules, as evidenced by the marked vacuolar degeneration and coagulative necrosis, as well as the presence of eosinophilic material and tubular casts within the lumens of the renal tubules, in addition to the infiltration of inflammatory cells, primarily neutrophils and macrophages. Section of **(D)** prunetin-treated I/R rats depicts mild congested renal blood vessels and slight vacuolar degeneration of the epithelial lining of some renal tubules. This improvement was canceled by the pre-administration of the blocker, where panel **(E)** reveals damage similar to that induced by I/R insult besides the congestion in renal blood vessels, major vacuolar degeneration, and coagulative necrosis of the epithelial lining of the renal tubules. All these effects are summarized in panel **(F)**, which represents the corresponding alterations in the scores of total histopathological lesions.

4. Discussion

Our study provided novel evidence of the therapeutic efficacy of prunetin, a naturally occurring methylated isoflavone, in mitigating I/R-induced AKI in rats for the first time. Here, we proved that prunetin acts by activating the membrane-bound estrogen receptor GPR30, where it upregulated its gene expression and content. Moreover, prunetin suppresses the inflammatory cascade of indoxyl sulfate/TLR4/TRIF. The prunetin-induced inhibition of the latter axis and the activation/normalization of caspase-8 were

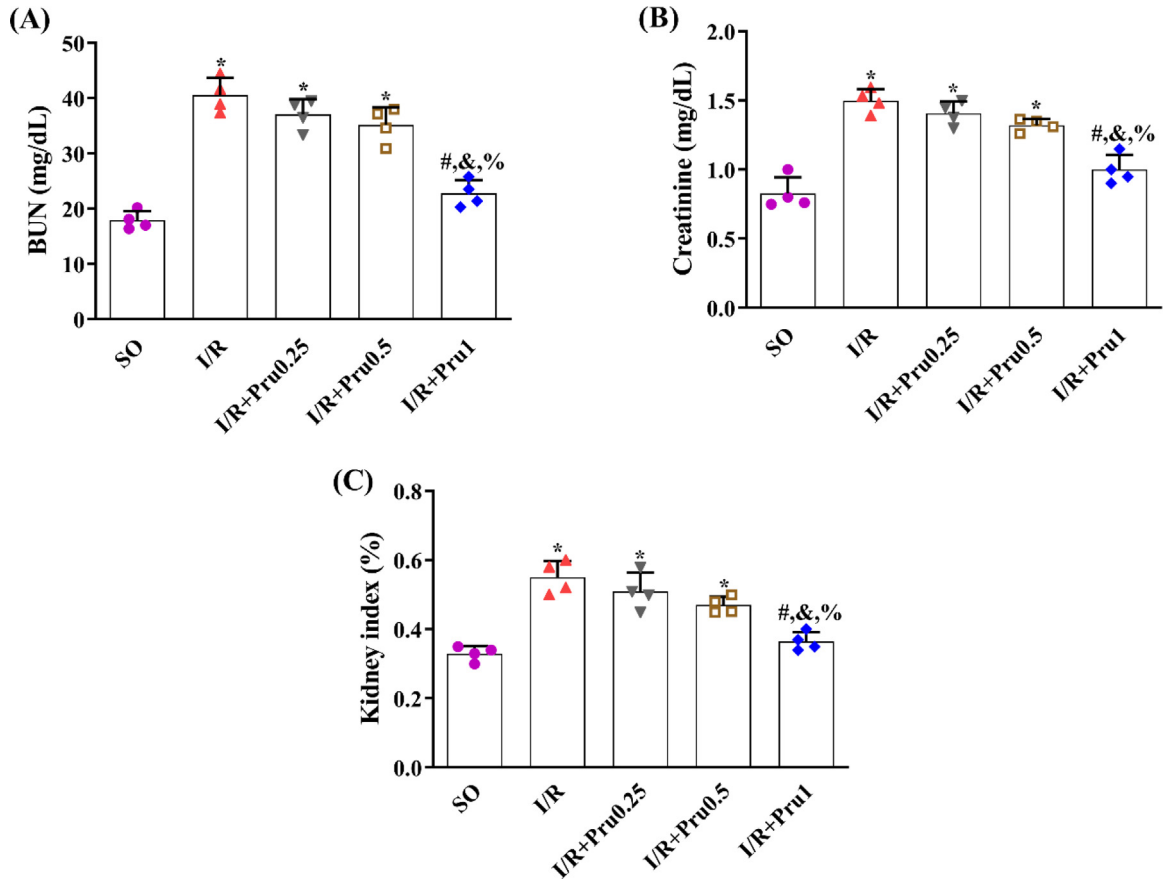

Fig. 1. The impact of different doses of prunetin on renal function biomarkers (A) BUN and (B) Creatinine, as well as (C) kidney index in rats with I/R. Rats underwent renal I/R and then received different doses of prunetin (0.25, 0.5, and 1 mg/kg, i.p.) once daily for three successive days. Data are displayed as mean ± SD (n = 4) and were statistically analyzed by one-way ANOVA followed by Tukey's post-hoc test ($P < 0.05$). *, #, &, or % denote comparisons to SO, I/R, Pru 0.25 mg/kg, or Pru 0.5 mg/kg-treated groups, respectively. **BUN:** Blood urea nitrogen; **I/R:** Ischemia/reperfusion; **Pru:** Prunetin; **SO:** Sham-operated.

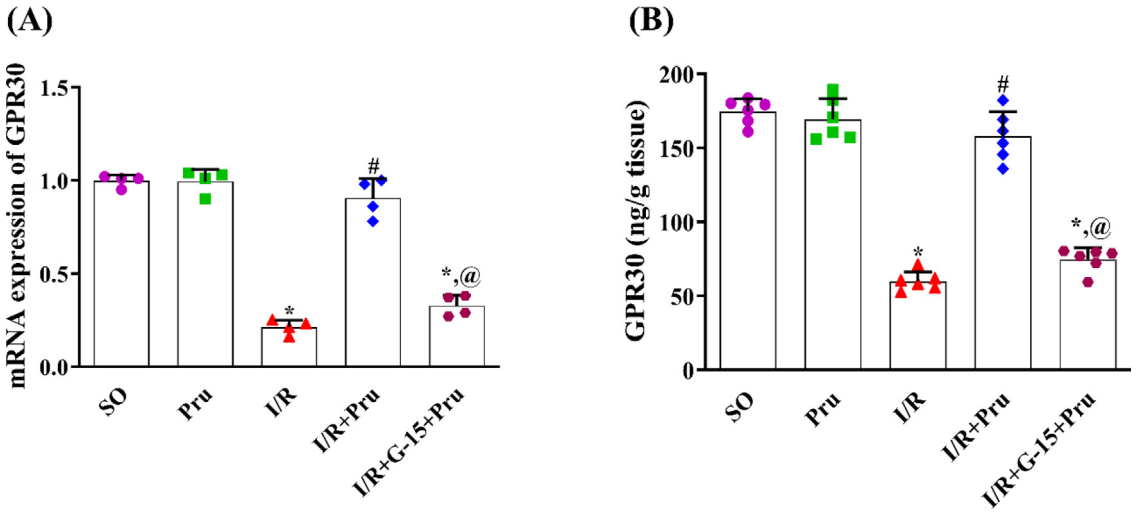

Fig. 2. Prunetin increased the (A) mRNA expression and (B) content of renal GPR30 in rats with I/R. Rats underwent renal I/R and then received a daily intraperitoneal injection of 1 mg/kg prunetin for three successive days alone or preceded by the GPR30 blocker, G-15. Data are displayed as mean ± SD (n = 4/6) and were statistically analyzed using one-way ANOVA followed by Tukey's post-hoc test ($P < 0.05$). *, #, or @ denote comparisons to SO, I/R, or I/R + Pru-treated groups, respectively. **GPR30:** G protein-coupled receptor 30; **I/R:** Ischemia/reperfusion; **Pru:** Prunetin; **SO:** Sham-operated.

responsible for the turned-off necroptotic trajectory evinced by the inhibited RIPK1/RIPK3/MLKL pathway. Additionally, prunetin hampered mitochondrial fission by decreasing the active RIPK3/PGMA5/DRP-1 cue (Fig. 7). Interrupting the crosstalk between these pathways improved the microscopic kidney structure and can be the reason why prunetin leveled off the elevated kidney function biomarkers. To prove our notion that activation of GPR30 is one of the prunetin reno-therapeutic mechanisms, our

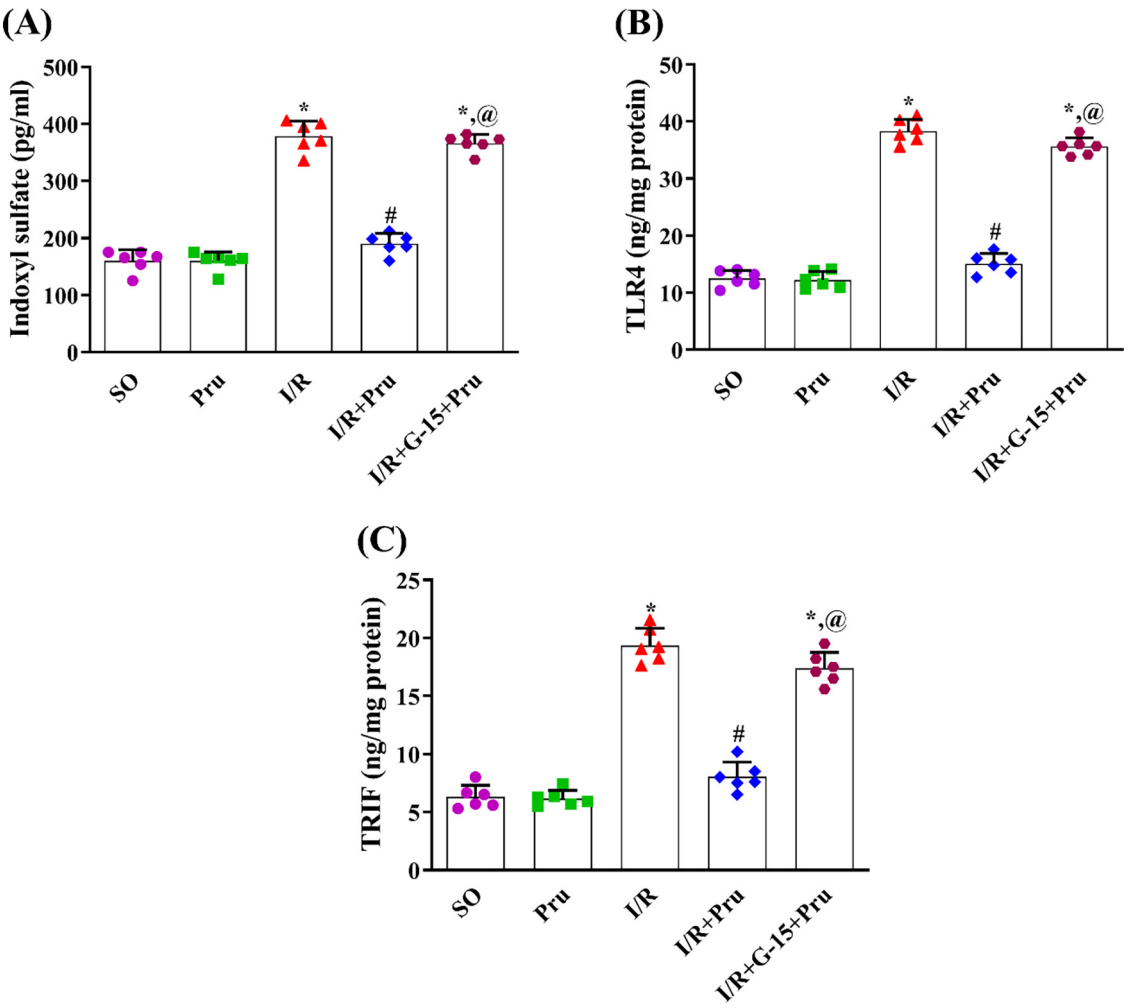

Fig. 3. Prunetin reduced serum level of (A) indoxyl sulfate and renal contents of (B) TLR4 and (C) TRIF in a GPR30-dependent manner in rats with I/R. Rats underwent renal I/R and then received a daily intraperitoneal injection of 1 mg/kg prunetin for three successive days alone or preceded by the GPR30 blocker, G-15. Data are displayed as mean ± SD (n = 6) and were statistically analyzed using one-way ANOVA followed by Tukey's post-hoc test ($P < 0.05$). *, #, or @ denote comparisons to SO, I/R, or I/R + Pru-treated groups, respectively. **I/R:** Ischemia/reperfusion; **Pru:** Prunetin; **SO:** Sham-operated; **TLR4:** Toll-like receptor 4; **TRIF:** toll/interleukin-1 receptor-domain-containing adaptor inducing interferon-beta.

results showed that all these improvements were canceled when the selective GPR30 blocker was administered before the injection of prunetin.

Here, we showed that prunetin alleviated the I/R-mediated enhancement of kidney function biomarkers. Although this dietary phytochemical was not tested before in AKI, biochanin A, another methylated isoflavone, improved these functional biomarkers in a cisplatin-induced kidney injury model (Suliman et al., 2018) to support our findings. Besides, the post-administration of prunetin has corrected the elevated renal index. This marker indicates I/R-induced renal hypertrophy that has a major role in models of kidney I/R injury (Chu et al., 2022) and renal I/R-induced brain injury (Azarkish et al., 2021).

This study also documented that the prunetin reno-therapeutic effect was mediated by activating the membrane-bound estrogen receptor GPR30, where it upregulated the mRNA expression of this receptor as well as its protein content. Previously, prunetin in an in-vitro study has improved bone regeneration by activating this receptor (Khan et al., 2015), a fact that braces prunetin as an activator of this receptor. By the same token, the isoflavone daidzein improved cerebellar development through the activation of GPR30 (Ariyani et al., 2019). These findings were further confirmed by the abolishment of the prunetin therapeutic effect when preceded by G-15 (GPR30 blocker) to concur with a former study in which the anti-inflammatory role of the biochanin A isoflavone was annulled by G-15 in the antigen-induced arthritis model (Felix et al., 2021). Indeed, the activation of GPR30 played a protective role in neuropathological disorders (Ariyani et al., 2019; Wu et al., 2018) and different kidney injury models other than I/R (Lindsey et al., 2011; Maric-Bilkan and Flynn, 2012). Here, we showed that the induction of the renal I/R model has markedly repressed both the mRNA expression and content of GPR30, an effect that mimics the findings of former studies in which various renal injury models have blunted the expression of this receptor (Buléon et al., 2020; Wang et al., 2020).

The I/R injurious ramification was verified by the doubled level of the uremic toxin indoxyl sulfate to harmonize with a former study (Wu et al., 2013). This toxin accumulates in the bloodstream due to a reduced glomerular filtration rate (Burek et al., 2020), as evidenced here by the serum elevation of BUN and creatinine. The increment of this uremic toxin acts as a conditional danger signal-associated molecular pattern that activates toll-like receptors, mainly TLR4 to consequently recruit/activate its intracellular adaptor protein, TRIF (Sun et al., 2018), verities that tone with our work, where both TLR4 and its adaptor were boosted here and *hitherto* (Kohansal et al., 2019; Paulus et al., 2014; Zhao

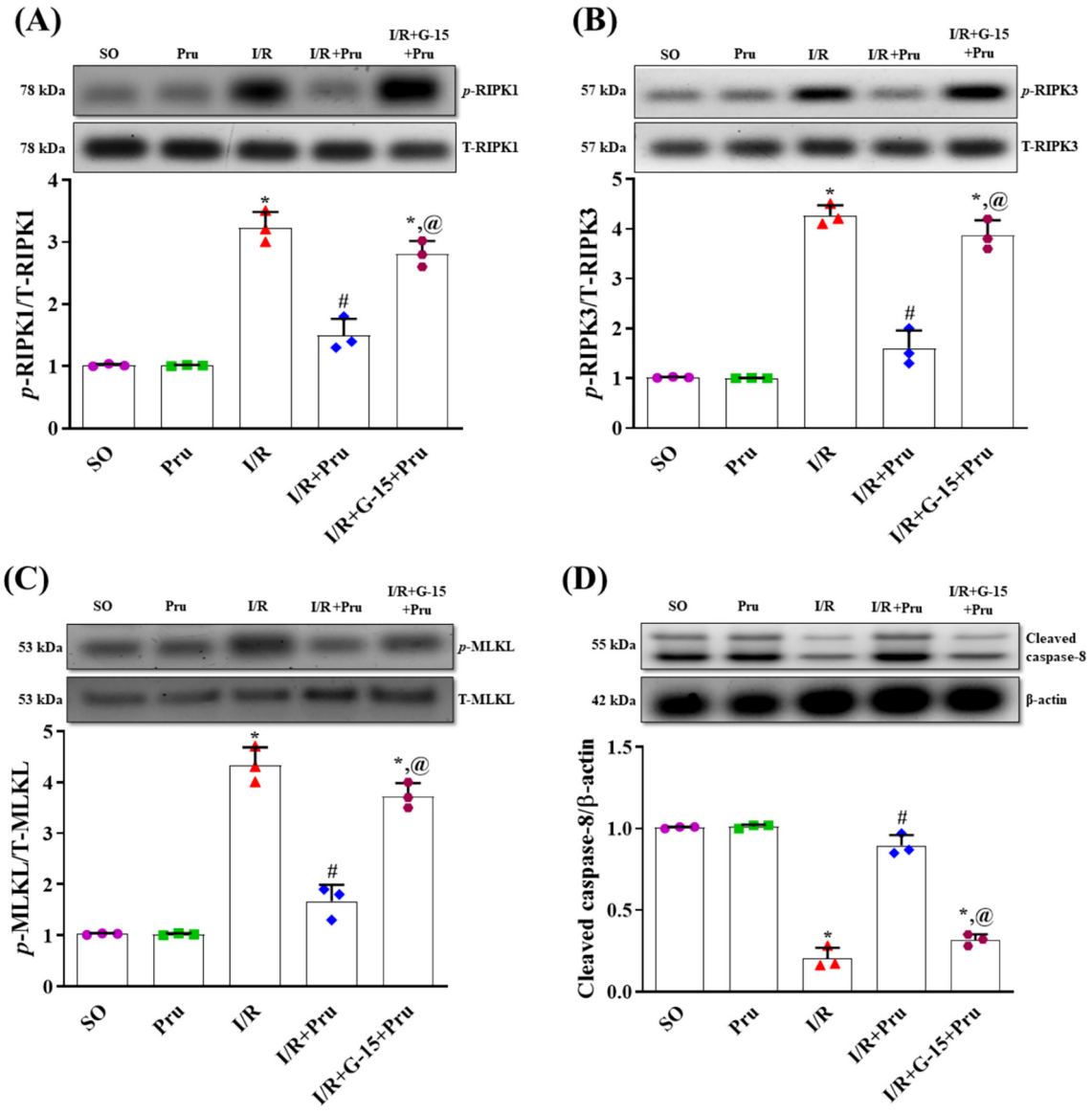

Fig. 4. Prunetin downregulated the protein expression of (A) *p*-RIPK1, (B) *p*-RIPK3, and (C) *p*-MLKL but upregulated that of (D) cleaved caspase-8 in rats with I/R. Rats underwent renal I/R and then received a daily intraperitoneal injection of 1 mg/kg prunetin for three successive days alone or preceded by the GPR30 blocker, G-15. Data are displayed as mean ± SD (n = 6) and were statistically analyzed using one-way ANOVA followed by Tukey's post-hoc test ($P < 0.05$). *, #, or @ denote comparisons to SO, I/R, or I/R + Pru-treated groups, respectively. **I/R:** Ischemia/reperfusion; **MLKL:** Mixed lineage kinase domain-like; ***p*:** Phosphorylated; **Pru:** Prunetin; **RIPK1/3:** Receptor-interacting protein kinase 1/3; **SO:** Sham-operated; **T:** total.

et al., 2014). Nevertheless, post-administration of prunetin has abated these elevations to highlight its anti-inflammatory effect, again, through the activation of GPR30, evidenced by the abolition of these favorable effects in the presence of G-15 to highlight the crosstalk between indoxyl sulfate/TLR4/TRIF and GPR30. Indeed, similar verdicts were presented by Zhang et al. (2018) who underlined the relation between TLR4 and GPR30 in the cerebral ischemia model and reported the downregulation of TLR4 expression in response to GPR30 activation.

Besides the inflammatory role, the indoxyl sulfate/TLR4/TRIF axis can initiate necroptosis by eliciting a cascade of events (Linkermann and Green, 2014). The current treatment with prunetin attested its survival anti-necroptotic activity, for the first time, by restoring caspase-8 and turning off the necroptotic signal through leveling off the protein expression of its chief regulatory proteins, *p*-RIPK1, *p*-RIPK3, and *p*-MLKL, thereby, contesting the I/R-induced necroptotic cue. Notably, GPR30 had again demonstrated its critical effect in explaining the anti-necroptotic role of prunetin, where the presence of G-15 before prunetin re-enhanced the protein expression of the active/phosphorylated necroptotic signaling pathway RIPK1/RIPK3/MLKL while mitigating that of caspase-8. A recent study using the hepatic I/R model braces this notion where activation of GPR30 inhibited the I/R-induced necroptosis to be cancelled by the pre-administration of G-15 (Li et al., 2022b).

The activation of the necrosome molecules during I/R injury expands their detrimental role, leading to mitochondrial dysfunction through the activation of PGAM5 to trigger the recruitment and activation of the mitochondrial fission factor DRP-1, ultimately promoting fragmentation of mitochondria. In this context, the necroptotic complex was formerly reported to stimulate PGAM5, resulting in the activation of DRP-1 with the subsequent impairment of mitochondria (Cheng et al., 2021). Furthermore, a recent study proved the significant reduction of the active

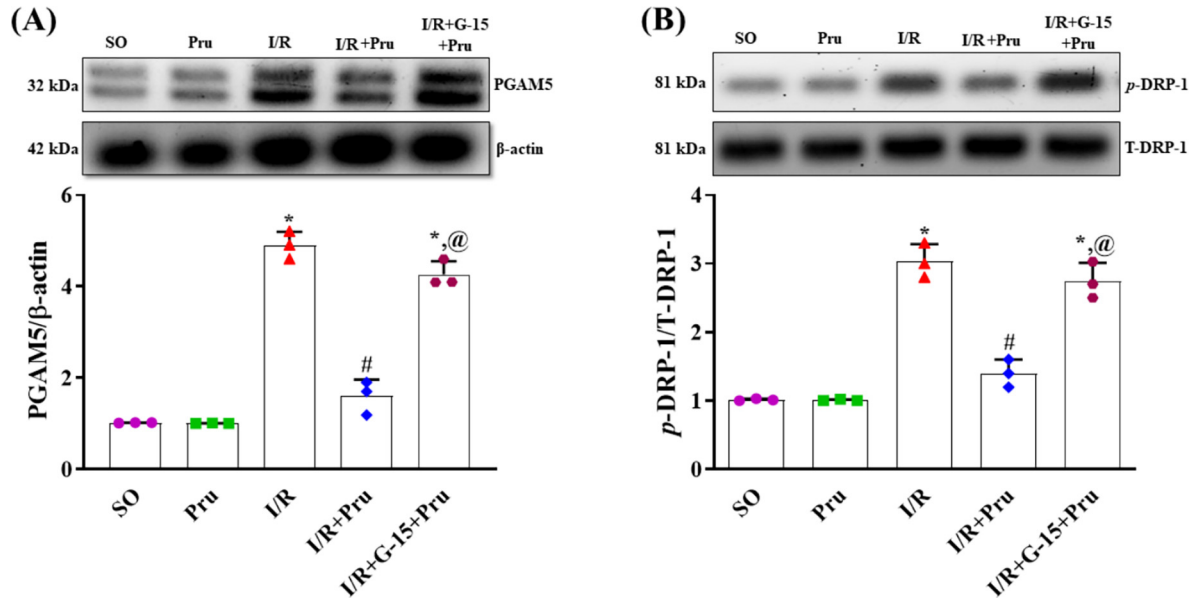

Fig. 5. Prunetin amended mitochondrial fission by downregulating the protein expression of (A) PGAM5 and (B) *p*-DRP-1 in rats with I/R. Rats underwent renal I/R and then received a daily intraperitoneal injection of 1 mg/kg prunetin for three successive days alone or preceded with the GPR30 blocker, G-15. Data are displayed as mean ± SD (n = 6) and were statistically analyzed using one-way ANOVA followed by Tukey's post-hoc test ($P < 0.05$). *, #, or @ denote comparisons to SO, I/R, or I/R + Pru-treated groups, respectively. **DRP-1:** Dynamin-related protein 1; **I/R:** Ischemia/reperfusion; ***p*:** Phosphorylated; **PGAM5:** Phosphoglycerate mutase 5; **Pru:** Prunetin; **SO:** Sham-operated; **T:** total.

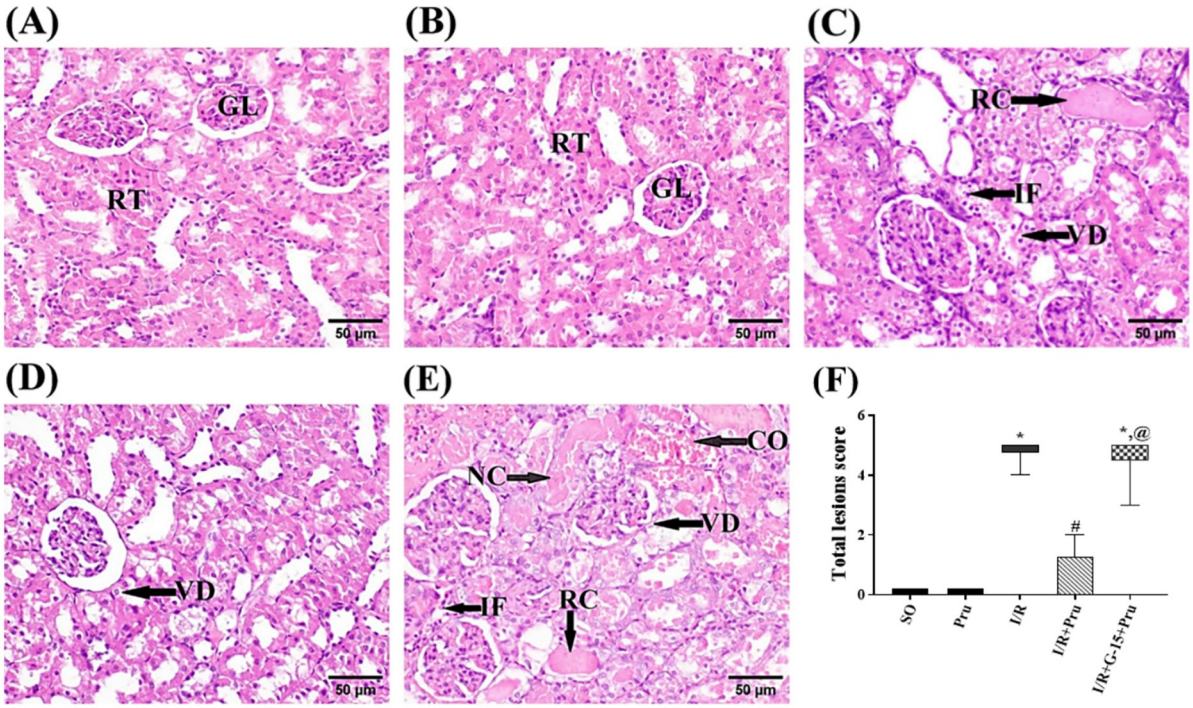

Fig. 6. Prunetin restored the altered histological structure of the kidney. Photomicrographs representing H&E-stained renal tissue sections of rats (scale bar 50 µm). Sections of the **(A)** SO and the **(B)** SO + Pru reveal the regular histological structure of renal parenchyma (normal glomeruli [GL] and renal tubules [RT]). Section of the **(C)** I/R group depicts marked changes in renal tubules manifested by epithelial lining vacuolar degeneration [VD], eosinophilic renal cast [RC] in the lumen, and inflammatory cell infiltration [IF]. Section of the **(D)** Pru-treated group reveals slight VD of some renal tubules, whereas the section of the **(E)** G-15 blocker group + Pru shows congestion of renal blood vessels [CO], marked VD, coagulative necrosis of renal tubular epithelium [NC], RC in the lumen of renal tubules, and IF. These data are recapitulated in panel **(F)**, which illustrates the total renal damage score in the different groups. The median (min–max) of 6 non-overlapping microscopic fields per animal (n = 3/group) was used to represent the non-parametric data, which were analyzed by the Kruskal-Wallis test followed by Dunn's post-hoc test ($P < 0.05$). *, #, or @ denote comparisons to SO, I/R, or I/R + Pru groups, respectively. **I/R:** Ischemia/reperfusion; **Pru:** Prunetin; **SO:** Sham-operated.

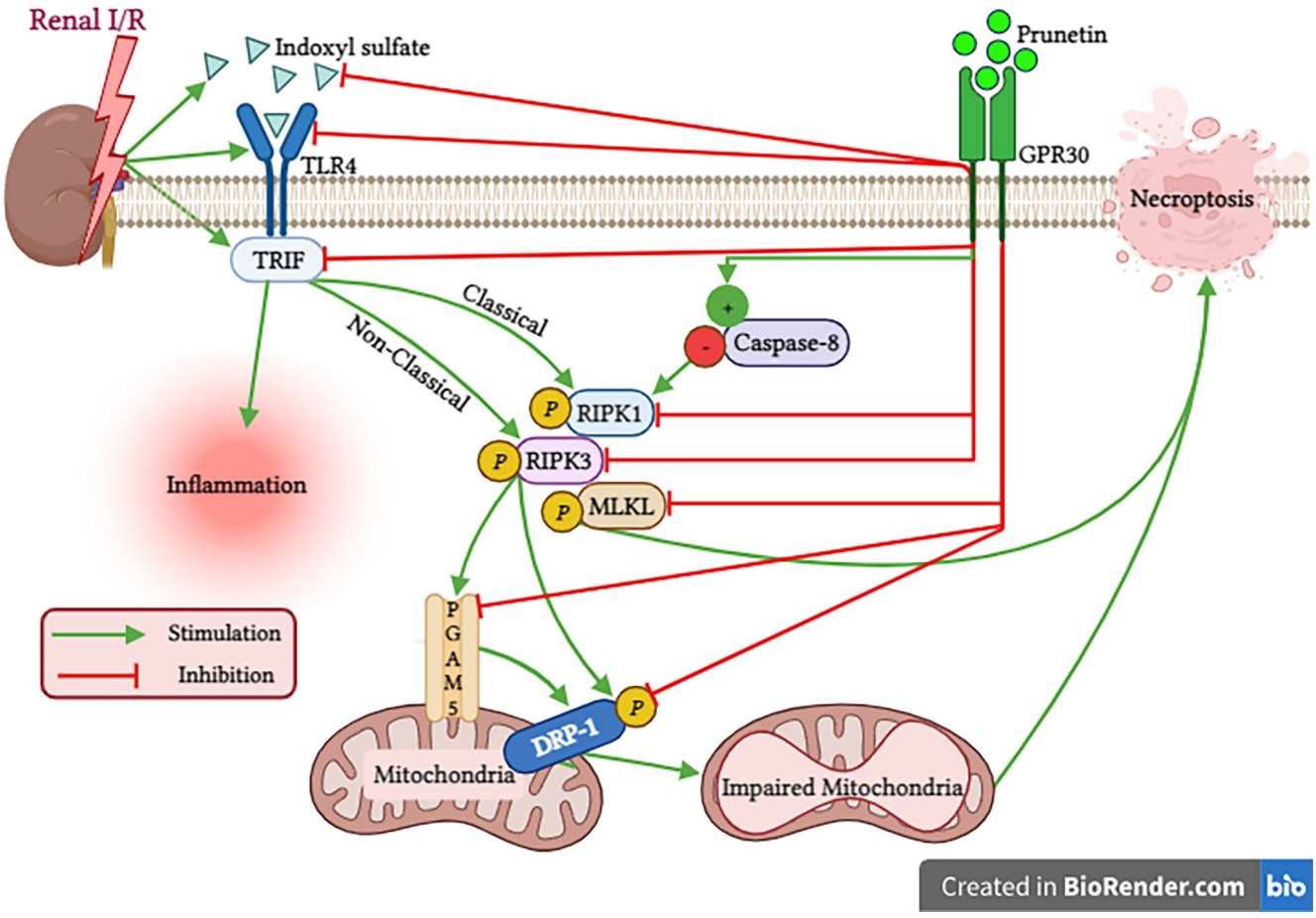

Fig. 7. Schematic presentation depicting molecular cascades involved in the reno-therapeutic effect of prunetin against I/R injury. Prunetin by activating GPR30 inhibits (1) the indoxyl sulfate/TLR4/TRIF inflammatory hub, (2) RIPK1/RIPK3/MLKL necroptotic trajectory, and (3) RIPK3/PGAM5/DRP-1 cue responsible for mitochondrial fission in the I/R kidney. **DRP-1:** Dynamin-related protein 1; **GPR30:** G protein-coupled receptor 30; **I/R:** Ischemia/Reperfusion; **MLKL:** Mixed lineage kinase domain-like; ***p*:** Phosphorylated; **PGAM5:** Phosphoglycerate mutase 5; **RIPK1/3:** Receptor-interacting protein kinase 1/3; **TLR4:** Toll-like receptor 4; **TRIF:** toll/interleukin-1 receptor-domain-containing adaptor inducing interferon-beta. This Fig. is created with BioRender.com.

p(ser616)-DRP-1 due to PGAM5 knockdown (Sang et al., 2023). Of note, activated RIPK3 can also directly activate/phosphorylate the mitochondrial fission executor, DRP-1 at the serine 616 site (Al-Lamki et al., 2016). The harmful effect of the currently activated RIPK3/PGAM5/DRP-1 cascade was also reported to mediate plasma membrane rupture and provoke solid organ injury (Wang et al., 2012; Zhao et al., 2015). In a vicious cycle, the PGAM5/DRP-1 axis can again initiate necroptosis to maintain the harmful cycle (Wang et al., 2012). Similarly, a study held in 2019 documented that inhibited PGAM5/DRP-1 cue abolished necroptosis in the cardiac I/R injury model (She et al., 2019). Recently, it was proven that the PGAM5-mediated pathway is a critical determinant of kidney injury and that targeting this axis may be useful for treating AKI (Li et al., 2022c). These verities reinforce the reno-therapeutic mechanism of prunetin, which, besides suppressing necroptosis, decreases the mitochondrial fission pathway. Furthermore, blockage of GPR30 by G-15 reversed the reduced PGAM5 and *p*-DRP-1 protein expressions mediated by prunetin administration, confirming that it maintained renal mitochondrial integrity and prevented renal deterioration through the activation of GPR30.

The crosstalk between the above-examined pathways explains the improved renal morphology achieved by treatment with prunetin, which majorly restored the normal architecture of the renal tissues and improved the I/R-induced major renal histopathological damage. These outcomes align with a recently conducted study revealing the ability of prunetin to protect hepatic tissues against diethylnitrosamine-induced hepatocellular cancer (Li et al., 2022a). In this context, GPR30 activation by prunetin is one possible mechanism of histological improvement, as approved herein, since pre-administration of G-15 markedly worsened this enhancement.

Study Limitations: The current study highlighted the role of G-15 in blocking the effect of GPR30 activation; however, its sole effect on kidney function and the assessed parameters was not evaluated in a separate group, which imposes a limitation on our study since the blocker could have off-target effects.

5. Conclusion

In the current work, we highlighted the therapeutic effect of prunetin against I/R-induced AKI in rats for the first time. This beneficial impact was in part mediated through the activation of GPR30 to suppress inflammation, necroptosis, and mitochondrial fission. These effects were confirmed by the abrogation of the inflammatory axis indoxyl sulfate/TLR4/TRIF, the repression of the activated/phosphorylated necroptotic cascade RIPK1/RIPK3/MLKL, and the inhibition of the activated mitochondrial fission cue RIPK3/PGMA5/DRP-1. However, these beneficial effects were nullified by the pre-administration of the GPR30 blocker G-15, which further highlights the role of GPR30 in the prunetin thera-

peutic effect. These results, thus, nominate prunetin as a promising nutraceutical against AKI. However, additional in-vivo and in-vitro studies await to elucidate further possible therapeutic mechanism (s) of prunetin in this model.

Declaration of Competing Interest

The authors declare that they have no known competing financial interests or personal relationships that could have appeared to influence the work reported in this paper.

Acknowledgment

The authors would like to thank "Future University in Egypt" for financially supporting the publication fees.

References

Abulfadl, Y., El-Maraghy, N., Ahmed, A.E., Nofal, S., Abdel-Mottaleb, Y., Badary, O.A., 2018. Thymoquinone alleviates the experimentally induced Alzheimer's disease inflammation by modulation of TLRs signaling. Hum. Exp. Toxicol. 37, 1092–1104. https://doi.org/10.1177/0960327118755256.

Al-Lamki, R., Lu, W., Manalo, P., Wang, J., Warren, A., Tolkovsky, A., Pober, J., Bradley, J., 2016. Tubular epithelial cells in renal clear cell carcinoma express high RIPK1/3 and show increased susceptibility to TNF receptor 1-induced necroptosis. Cell Death & Disease 7, e2287.

Ariyani, W., Miyazaki, W., Koibuchi, N., 2019. A novel mechanism of s-equol action in neurons and astrocytes: the possible involvement of GPR30/GPER1. Int. J. Mol. Sci. 20, 5178. https://doi.org/10.3390/ijms20205178.

Azarkish, F., Armin, F., Ab Parvar, A.A., Dehghani, A., 2021. The influence of renal ischemia-reperfusion injury on remote organs: The histological brain changes in male and female rats. Brain Circ. 7, 194–200. https://doi.org/10.4103/bc.bc_3_21.

Belizario, J., Vieira-Cordeiro, L., Enns, S., 2015. Necroptotic cell death signaling and execution pathway: lessons from knockout mice. Mediators Inflamm. 2015,. https://doi.org/10.1155/2015/128076.12807 128076.

Bonventre, J.V., Weinberg, J.M., 2003. Recent advances in the pathophysiology of ischemic acute renal failure. J. Am. Soc. Nephrol. 14, 2199–2210. https://doi.org/10.1097/01.ASN.0000079785.

Buléon, M., Cuny, M., Grellier, J., Charles, P., Belliere, J., Casemayou, A., Arnal, J., Schanstra, J., Tack, I., 2020. A single dose of estrogen during hemorrhagic shock protects against kidney injury whereas estrogen restoration in ovariectomized mice is ineffective. Sci. Rep. 10, 17240. https://doi.org/10.1038/s41598-020-73974-5.

Burek, M., Burmester, S., Salvador, E., Möller-Ehrlich, K., Schneider, R., Roewer, N., Nagai, M., Förster, C.Y., 2020. Kidney ischemia/reperfusion injury induces changes in the drug transporter expression at the blood-brain carrier in vivo and in vitro. Front. Physiol. 11,. https://doi.org/10.3389/fphys.2020.569881 569881.

Carmeci, C., Thompson, D.A., Ring, H.Z., Francke, U., Weigel, R.J., 1997. Identification of a gene (GPR30) with homology to the G-protein-coupled receptor superfamily associated with estrogen receptor expression in breast cancer. Genomics 45, 607–617. https://doi.org/10.1006/geno.1997.4972.

Chang, Y., Han, Z., Zhang, Y., Zhou, Y., Feng, Z., Chen, L., Li, X., Li, L., Si, J., 2019. G protein-coupled estrogen receptor activation improves contractile and diastolic functions in rat renal interlobular artery to protect against renal ischemia reperfusion injury. Biomed. Pharmacother. 112,. https://doi.org/10.1016/j.biopha.2019.108666 108666.

Cheng, M., Lin, N., Dong, D., Ma, J., Su, J., Sun, L., 2021. PGAM5: a crucial role in mitochondrial dynamics and programmed cell death. Eur. J. Cell Biol. 100,. https://doi.org/10.1016/j.ejcb.2020.151144 151144.

Chu, C., Delić, D., Alber, J., Feger, M., Xiong, Y., Luo, T., Hasan, A.A., Zeng, S., Gaballa, M.M.S., Chen, X., Yin, L., Klein, T., Elitok, S., Krämer, B.K., Föller, M., Hocher, B., 2022. Head-to-head comparison of two SGLT-2 inhibitors on AKI outcomes in a rat ischemia-reperfusion model. Biomed. Pharmacother. 153,. https://doi.org/10.1016/j.biopha.2022.113357 113357.

Dhuriya, Y.K., Sharma, D., 2018. Necroptosis: a regulated inflammatory mode of cell death. J. Neuroinflamm. 15, 199. https://doi.org/10.1186/s12974-018-1235-0.

Felix, F.B., Vago, J.P., Fernandes, D.D.O., Martins, D.G., Moreira, I.Z., Gonçalves, W.A., Costa, W.C., Araújo, J.M.D., Queiroz-Junior, C.M., Campolina-Silva, G.H., 2021. Biochanin A regulates key steps of inflammation resolution in a model of antigen-induced arthritis via GPR30/PKA-dependent mechanism. Front. Pharmacol. 12,. https://doi.org/10.3389/fphar.2021.662308 662308.

Grootjans, S., Vanden Berghe, T., Vandenabeele, P., 2017. Initiation and execution mechanisms of necroptosis: an overview. Cell Death Differ. 24, 1184–1195. https://doi.org/10.1038/cdd.2017.65.

Habib, R., 2021. Multifaceted roles of Toll-like receptors in acute kidney injury. Heliyon 7, e06441.

Holler, N., Zaru, R., Micheau, O., Thome, M., Attinger, A., Valitutti, S., Bodmer, J., Schneider, P., Seed, B., Tschopp, J., 2000. Fas triggers an alternative, caspase-8–independent cell death pathway using the kinase RIP as effector molecule. Nat. Immunol. 1, 489–495. https://doi.org/10.1038/82732.

Hu, H., Li, H., 2018. Prunetin inhibits lipopolysaccharide-induced inflammatory cytokine production and MUC5AC expression by inactivating the TLR4/MyD88 pathway in human nasal epithelial cells. Biomed. Pharmacother. 106, 1469–1477. https://doi.org/10.1016/j.biopha.2018.07.093.

Hutchens, M.P., Nakano, T., Kosaka, Y., Dunlap, J., Zhang, W., Herson, P.S., Murphy, S. J., Anderson, S., Hurn, P.D., 2010. Estrogen is renoprotective via a nonreceptor-dependent mechanism after cardiac arrest in vivo. Anesthesiology 112, 395–405. https://doi.org/10.1097/ALN.0b013e3181c98da9.

Jun, W., Benjanuwattra, J., Chattipakorn, S.C., Chattipakorn, N., 2020. Necroptosis in renal ischemia/reperfusion injury: a major mode of cell death? Arch. Biochem. Biophys. 689,. https://doi.org/10.1016/j.abb.2020.108433 108433.

Khan, K., Pal, S., Yadav, M., Maurya, R., Trivedi, A.K., Sanyal, S., Chattopadhyay, N., 2015. Prunetin signals via G-protein-coupled receptor, GPR30 (GPER1): stimulation of adenylyl cyclase and cAMP-mediated activation of MAPK signaling induces Runx2 expression in osteoblasts to promote bone regeneration. J. Nutr. Biochem. 26, 1491–1501. https://doi.org/10.1016/j.jnutbio.2015.07.021.

Kohansal, P., Rajai, N., Dehpour, A.R., Rashidian, A., Shafaroodi, H., 2019. The protective effect of acute pantoprazole pretreatment on renal ischemia/reperfusion injury in rats. Fundam. Clin. Pharmacol. 33, 405–411. https://doi.org/10.1111/fcp.12451.

Lattanzio, M.R., Kopyt, N.P., 2009. Acute kidney injury: new concepts in definition, diagnosis, pathophysiology, and treatment. J. Osteopath. Med. 109, 13–19. https://doi.org/10.7556/jaoa.2009.109.1.13.

Li, Z., Chen, L., Chu, H., Wang, W., Yang, L., 2022b. Estrogen alleviates hepatocyte necroptosis depending on GPER in hepatic ischemia reperfusion injury. J. Physiol. Biochem. 78, 125–137. https://doi.org/10.1007/s13105-021-00846-5.

Li, G., Qi, L., Chen, H., Tian, G., 2022a. Involvement of NF-κB/PI3K/AKT signaling pathway in the protective effect of prunetin against a diethylnitrosamine induced hepatocellular carcinogenesis in rats. J. Biochem. Mol. Toxicol. 36, e23016.

Li, J., Sun, X., Yang, N., Ni, J., Xie, H., Guo, H., Wang, X., Zhou, L., Liu, J., Chen, S., Wang, X., Zhang, Y., Yu, C., Zhang, W., Lu, L., 2022c. Phosphoglycerate mutase 5 initiates inflammation in acute kidney injury by triggering mitochondrial DNA release by dephosphorylating the pro-apoptotic protein Bax. Kidney Int. 103, 115–133. https://doi.org/10.1016/j.kint.2022.08.022.

Lindsey, S.H., Yamaleyeva, L.M., Brosnihan, K.B., Gallagher, P.E., Chappell, M.C., 2011. Estrogen receptor GPR30 reduces oxidative stress and proteinuria in the salt-sensitive female mRen2.Lewis rat. Hypertension 58, 665–671. https://doi.org/10.1161/hypertensionaha.111.175174.

Linkermann, A., Green, D.R., 2014. Necroptosis. N. Engl. J. Med. 370, 455–465. https://doi.org/10.1056/nejmra1310050.

Linkermann, A., Bräsen, J.H., Himmerkus, N., Liu, S., Huber, T.B., Kunzendorf, U., Krautwald, S., 2012. Rip1 (receptor-interacting protein kinase 1) mediates necroptosis and contributes to renal ischemia/reperfusion injury. Kidney Int. 81, 751–761. https://doi.org/10.1038/ki.2011.450.

Liu, T., Zong, H., Chen, X., Li, S., Liu, Z., Cui, X., Jia, G., Shi, Y., 2022. Toll-like receptor 4-mediated necroptosis in the development of necrotizing enterocolitis. Pediatr. Res. 91, 73–82. https://doi.org/10.1038/s41390-021-01457-y.

Lu, Y., Jiang, Q., Yu, L., Lu, Z., Meng, S., Su, D., Burnstock, G., Ma, B., 2013. 17β-estradiol rapidly attenuates P2X3 receptor-mediated peripheral pain signal transduction via ERα and GPR30. Endocrinology 154, 2421–2433. https://doi.org/10.1210/en.2012-2119.

Mansour, S.M., Abd El-Aal, S.A., El-Abhar, H.S., Ahmed, K.A., Awny, M.M., 2022. Repositioning of ticagrelor: renoprotection mediated by modulating renin-angiotensin system, inflammation, autophagy and galectin-3. Eur. J. Pharmacol. 918,. https://doi.org/10.1016/j.ejphar.2022.174793 174793.

Maric-Bilkan, C., Flynn, E., 2012. Activation of the novel estrogen receptor GPR30 reduces blood pressure and renal injury in the streptozotocin (STZ)-induced diabetic rat infused with angiotensin II. FASEB J. 26 (1096), 1.

Mutha, R.E., Tatiya, A.U., Surana, S.J., 2021. Flavonoids as natural phenolic compounds and their role in therapeutics: an overview. Future J. Pharm. Sci. 7, 25. https://doi.org/10.1186/s43094-020-00161-8.

Nih, O., Oer, O., 2011. Guide for the care and use of laboratory animals. In: Crossgrove, R., Fletcher, C.H. (Eds.), Committee for the Update of the Guide for the Care and Use of Laboratory Animals Institute for Laboratory Animal Research Division on Earth and Life Studies. The National Academies Press, Washington, pp. 1–246.

Nuransoy, A., Beytur, A., Polat, A., Samdanci, E., Sagir, M., Parlakpinar, H., 2015. Protective effect of sitagliptin against renal ischemia reperfusion injury in rats. Renal Fail. 37, 687–693. https://doi.org/10.3109/0886022X.2015.1010991.

Park, M.Y., Ha, S.E., Vetrivel, P., Kim, H.H., Bhosale, P.B., Abusaliya, A., Kim, G.S., 2021. Differences of key proteins between apoptosis and necroptosis. Biomed. Res. Int. 2021, 3420168. https://doi.org/10.1155/2021/3420168.

Paulus, P., Rupprecht, K., Baer, P., Obermüller, N., Penzkofer, D., Reissig, C., Scheller, B., Holfeld, J., Zacharowski, K., Dimmeler, S., 2014. The early activation of toll-like receptor (TLR)-3 initiates kidney injury after ischemia and reperfusion. PLoS One 9, e94366.

Prossnitz, E.R., Maggiolini, M., 2009. Mechanisms of estrogen signaling and gene expression via GPR30. Mol. Cell. Endocrinol. 308, 32–38. https://doi.org/10.1016/j.mce.2009.03.026.

Ragab, D., Abdallah, D.M., El-Abhar, H.S., 2014. Cilostazol renoprotective effect: Modulation of PPAR-γ, NGAL, KIM-1 and IL-18 underlies its novel effect in a model of ischemia-reperfusion. PLoS One 9, e95313.

Ren, L., Li, F., Di, Z., Xiong, Y., Zhang, S., Ma, Q., Bian, X., Lang, Z., Ye, Q., Wang, Y., 2022. Estradiol ameliorates acute kidney ischemia-reperfusion injury by inhibiting the TGF-βRI-SMAD pathway. Front. Immunol. 13,. https://doi.org/10.3389/fimmu.2022.822604 822604.

Sang, D., Duan, X., Yu, X., Zang, J., Liu, L., Wu, G., 2023. PGAM5 regulates DRP1-mediated mitochondrial fission/mitophagy flux in lipid overload-induced renal tubular epithelial cell necroptosis. Toxicol. Lett. 372, 14–24. https://doi.org/10.1016/j.toxlet.2022.10.003.

Satake, A., Takaoka, M., Nishikawa, M., Yuba, M., Shibata, Y., Okumura, K., Kitano, K., Tsutsui, H., Fujii, K., Kobuchi, S., Ohkita, M., Matsumura, Y., 2008. Protective effect of 17beta-estradiol on ischemic acute renal failure through the PI3K/Akt/eNOS pathway. Kidney Int. 73, 308–317. https://doi.org/10.1038/sj.ki.5002690.

She, L., Tu, H., Zhang, Y., Tang, L., Li, N., Ma, Q., Liu, B., Li, Q., Luo, X., Peng, J., 2019. Inhibition of phosphoglycerate mutase 5 reduces necroptosis in rat hearts following ischemia/reperfusion through suppression of dynamin-related protein 1. Cardiovasc. Drugs Ther. 33, 13–23. https://doi.org/10.1007/s10557-018-06848-8.

Shiva, N., Sharma, N., Kulkarni, Y.A., Mulay, S.R., Gaikwad, A.B., 2020. Renal ischemia/reperfusion injury: an insight on in vitro and in vivo models. Life Sci. 256,. https://doi.org/10.1016/j.lfs.2020.117860 117860.

Suliman, F.A., Khodeer, D.M., Ibrahiem, A., Mehanna, E.T., El-Kherbetawy, M.K., Mohammad, H.M.F., Zaitone, S.A., Moustafa, Y.M., 2018. Renoprotective effect of the isoflavonoid biochanin A against cisplatin induced acute kidney injury in mice: Effect on inflammatory burden and p53 apoptosis. Int. Immunopharmacol. 61, 8–19. https://doi.org/10.1016/j.intimp.2018.05.010.

Sun, Y., Johnson, C., Zhou, J., Wang, L., Li, Y., Lu, Y., Nanayakkara, G., Fu, H., Shao, Y., Sanchez, C., 2018. Uremic toxins are conditional danger-or homeostasis-associated molecular patterns. Front. Biosci. (landmark Ed.) 23, 348–387. https://doi.org/10.2741/4595.

Wang, Z., Jiang, H., Chen, S., Du, F., Wang, X., 2012. The mitochondrial phosphatase PGAM5 functions at the convergence point of multiple necrotic death pathways. Cell 148, 228–243. https://doi.org/10.1016/j.cell.2011.11.030.

Wang, H., Sun, L., Su, L., Rizo, J., Liu, L., Wang, L., Wang, F., Wang, X., 2014. Mixed lineage kinase domain-like protein MLKL causes necrotic membrane disruption upon phosphorylation by RIP3. Mol. Cell 54, 133–146. https://doi.org/10.1016/j.molcel.2014.03.003.

Wang, S., Zeng, M., Li, B., Kan, Y., Zhang, B., Zheng, X., Feng, W., 2020. Raw and salt-processed Achyranthes bidentata attenuate LPS-induced acute kidney injury by inhibiting ROS and apoptosis via an estrogen-like pathway. Biomed. Pharmacother. 129,. https://doi.org/10.1016/j.biopha.2020.110403 110403.

Wu, V., Young, G., Huang, P., Lo, S., Wang, K., Sun, C., Liang, C., Huang, T., Chen, J., Chang, F., Chen, Y., Kuo, Y., Chen, J., Chen, J., Chen, Y., Ko, W., Wu, K., The NSARF group, 2013. In acute kidney injury, indoxyl sulfate impairs human endothelial progenitor cells: modulation by statin. Angiogenesis. 16, 609-624. https://doi.org/10.1007/s10456-013-9339-8.

Wu, Y., Feng, D., Lin, J., Qu, Y., He, S., Wang, Y., Gao, G., Zhao, T., 2018. Downregulation of G-protein-coupled receptor 30 in the hippocampus attenuates the neuroprotection of estrogen in the critical period hypothesis. Mol. Med. Rep. 17, 5716–5725. https://doi.org/10.3892/mmr.2018.8618.

Yang, G., Ham, I., Choi, H., 2013. Anti-inflammatory effect of prunetin via the suppression of NF-κB pathway. Food Chem. Toxicol. 58, 124–132. https://doi.org/10.1016/j.fct.2013.03.039.

Zhang, Z., Qin, P., Deng, Y., Ma, Z., Guo, H., Guo, H., Hou, Y., Wang, S., Zou, W., Sun, Y., 2018. The novel estrogenic receptor GPR30 alleviates ischemic injury by inhibiting TLR4-mediated microglial inflammation. J. Neuroinflamm. 15, 206. https://doi.org/10.1186/s12974-018-1246-x.

Zhao, H., Perez, J.S., Lu, K., George, A.J., Ma, D., 2014. Role of toll-like receptor-4 in renal graft ischemia-reperfusion injury. Am. J. Physiol. Renal Physiol. 306, 801–811. https://doi.org/10.1152/ajprenal.00469.2013.

Zhao, H., Jaffer, T., Eguchi, S., Wang, Z., Linkermann, A., Ma, D., 2015. Role of necroptosis in the pathogenesis of solid organ injury. Cell Death Dis. 6, e1975.

Zimmerman, M.A., Budish, R.A., Kashyap, S., Lindsey, S.H., 2016. GPER-novel membrane oestrogen receptor. Clin. Sci. 130, 1005–1016. https://doi.org/10.1042/cs20160114.